Numeric modelling of a compact high temperature heat exchanger

Th. Fend, O. Smirnova, D. Schöllgen
German Aerospace Center, Institute of Solar Research, 51147 Köln , Linder Höhe, Germany
*E-Mail mailto: olena.smirnova.@dlr.de; Telephone +49 2203 601-2901

Abstract

The numeric investigations of a high temperature compact gas/gas heat exchanger are shown in this paper. The results of the numeric modelling and their analysis for two different simulation models with and without the regards of the development of the velocity field are presented in the article. The results have been obtained for two different geometries one of which is the two semi-channels model and second of which regards the heat transfer through the heat exchanger volume. The article presents the comparison of the model solutions with the evaluation of the received reliability results. The comparison between the simulations and experimental results are presented too. On the base of the second numeric model the two-dimensional simulation task with the regard of the inlet and outlet volume before and after the heat exchanger was developed. The influence of the change of the channel sizes on the hydraulic and thermal characteristics of the researched heat exchanger is shown. The solution of this two dimensional model confirms the inhomogeneous distribution of the hydraulic and thermal fields in the heat exchanger. The obtained results were analyzed with the conclusions and further investigations complete the represented results. "COMSOL-Multiphysics" was used for the numeric simulation.

Keywords: compact heat exchanger, heat transfer coefficient, high temperature, heat carrier

1. Introduction

The main aim of the numeric work was the creation and development of the models of the compact heat exchanger for the more detail investigation of the hydraulic and thermal fields in the heat exchanger which were obtained in the work at the project 3DKeST ("Three dimensional ceramic structures for the innovative applications"). The compact heat exchanger from extruded silicon carbide (SiC) was researched for use in high temperature applications. One possible application can be in the automobile industry as an energy saver, which supports the regeneration process of the particle filter. Thanks to its material properties such a heat exchanger can work at temperatures of up to 1200°C. The first test sample was realized using the counter flow principle.. The characteristics of this heat exchanger such as the heat transfer coefficient and the thermal efficiency have been obtained for different working parameters in previous experimental studies [1].

The researched heat exchanger was made of extruded silicon carbide (SiC) as a cylindrical body. The inner structure consists of quadratic channels. Each second row of these channels was closed from the frontal side after they have been slotted. In this way lateral openings are generated for these rows of channels. The heat carrier flow passes through these slots and moves through the channels which were closed from the frontal side. The second group of channels may be directly entered from the frontal side. In the further course of the text, they will be called "direct opened" channels. The channels to be entered from the slots will be called "slotted" channels correspondingly. A photo of the heat exchanger is presented in Figure 1. The flow path is illustrated in Figure 2.

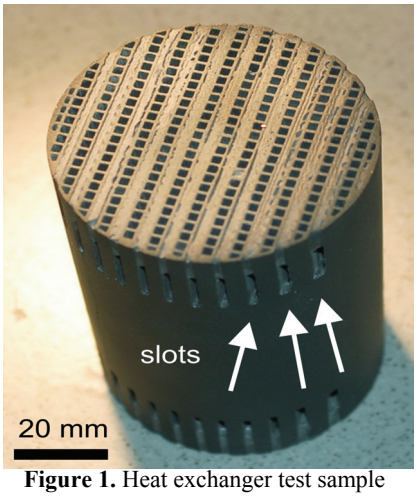

Figure 1. Heat exchanger test sample

The experimental results received showed some advantages of the investigated heat exchanger in comparison with other modern compact heat exchangers [3-6]. The experimental results raised the interest in numeric investigations of the temperature and velocity fields in this heat exchanger. The numeric work was divided into two models. One of which simulates only the heat flow at a constant velocity; the other regards the development of the hydraulic field together with the thermal field in the counter flow heat exchanger. The numeric simulation has the following aims:

1. Determination the velocity and thermal fields in the studied compact heat exchanger.

2. Determination of the influence of the geometry change and of the inlet cross–section change on the velocity and temperature fields.
The schematic moving of the fluxes is shown in Figure 2. Figure 2 (a) shows the scheme of the heat carrier flow through the "direct opened" channels; Figure 2 (b) additional shows the scheme of fluids movement in the researched counter flow heat exchanger.

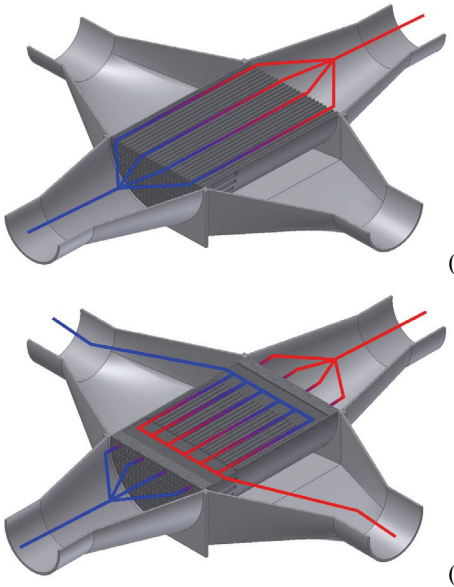

(a)

(b)

Figure 2. The schematic motion of the heat carrier flows through the studied heat exchanger.

2. Methodology

Two independent models have been taken for the simulation. The first model only regards the heat transfer at constant velocity; the second model regards both hydrodynamics and heat transfer.

Heat exchanger model at constant velocity

This model is presented in the "Heat Transfer Module (User's Guide)" for the COMSOL 3.4 [2]. The model yields a solution of the heat-transport problem with constant velocity in the main flow direction. Later, the model will be named as the one-variable model.

Heat exchanger model regarding of the velocity field

This model consists of the two following COMSOL modules: 1. weakly compressible Navies–Stokes; 2. general heat transfer non–isothermal flow. The second model gives the solution along the channel's length and along the channel's cross–section therefore below it will be called "two-variables model". The area and boundary conditions for this model are shown in Table 1.

Module	Area	Boundary conditions		
		conditions	**Inlet**	**Outlet**
Weakly compr. Navier - Stokes		$\nabla p = \nabla \eta \cdot \left(\nabla u + (\nabla u)^T\right)$ $\nabla u = 0$	Velocity $u = u_0$	Pressure without viscose stress $p = p_0$
General Heat Transfer (htgh)		$\nabla(-k \cdot \nabla T) + \rho \cdot c_p \cdot u \cdot \nabla T = 0$	Tempe-rature $T = T_0$	Convek. Fluss $n(-k \cdot \nabla T) =$

Table 1: Area and boundary conditions

The main geometry characteristics of the heat exchanger samples are presented in Table 2. The value of the inlet velocity for the simulation was determined from the continuity equation of the porous body: $u_{inlet} = \frac{m}{\rho_i \cdot \pi \cdot D^2 \cdot \varepsilon}$, (1)

here ρ_i is the density of the medium, D is the diameter of the sample and ε is the porosity of the sample.

Sample	Channel's cross – section [m]	Wall thickness [m]	Porosity [%]
1	0,002	0,0008	42
2	0,00217	0,00058	53

Table 2: Heat exchanger dimensions

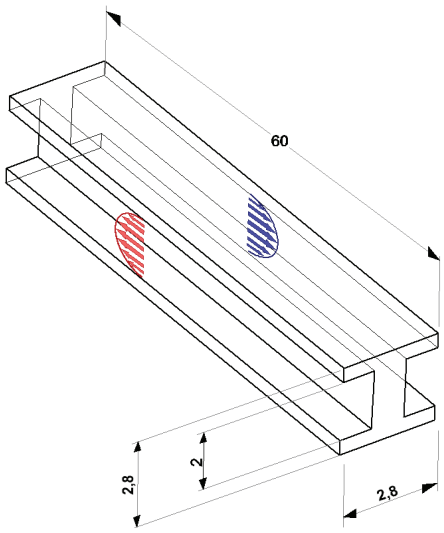

Figure 3. Geometry of the two semi-channels calculated with the one-variable model

The model was calculated for two different structures of the heat exchanger. Figure 3 shows the geometry of the coarse structure. Additionally, different inlet parameters such as the inlet air temperature and the inlet air velocity have been considered. The numeric solutions for the above described models were divided into two tasks. The two semi–channels was the first task and the full geometry was the second task. The second task was solved only for the active volume of the heat transfer between the heat carriers. In- and outlet

regions have been omitted. The second task was solved only with the first model because of the PC memory capacity limitation.

On the base of the second model an additional task was solved. This task was calculated in 2D. It has taken into account also the in- and outlet regions of the canning. Because of the geometry difference the 2D task was divided into 2 independent parts the "direct opened" channels and the slotted channels, both of them have been treated separately. Because of this each of the simulation tasks only included one heat carrier. For the influence of the other one a term "volumetric heat source" was used. The value of which was determined through the experimental specific heat flux:

$$q = \frac{Q}{N \cdot a^2 \cdot l} \qquad (2)$$

here $Q = m \cdot c_P \cdot \Delta T$ is the experimental heat flux, *a, l* und *N* are the width, length and quantity of the channels correspondingly. The common equation of the "General Heat Transfer" modus for this task is:

$$\nabla(-k \cdot \nabla T) + \rho \cdot c_p \cdot u \cdot \nabla T = \frac{Q}{N \cdot a^2 \cdot l} \qquad (3)$$

3. Results

The numeric solutions for the first model were obtained for both geometries with the two semi–channels and with the active heat transfer volume of the heat exchanger. One of the obtained solutions for both geometries is shown in Figure 4.

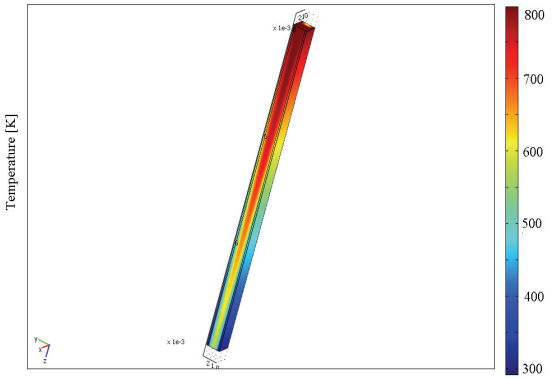

Figure 4(a) The simulation solution for the two semi–channels (one-variable-model)

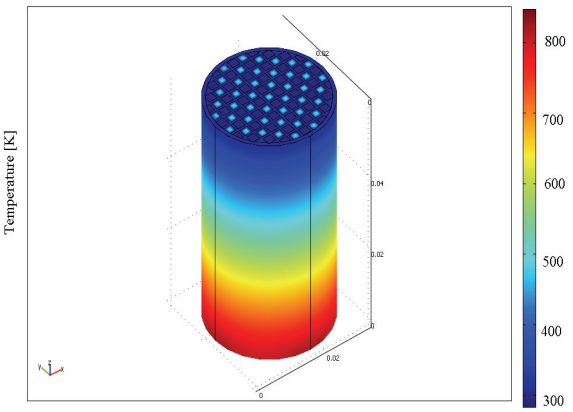

Figure 4(b) The simulation solution for the active volume of the heat exchanger

The results' analysis has the following goals:

1 The comparison of the both numeric models.

2 The determination of the influence of the channel sizes on the heat exchanger's characteristics.

These aims could be reached by the following steps:

1. The comparison of the numeric solutions of the above described two numeric models for one of the sample.
2. The comparison of the numeric solutions for two samples of one simulation model.

The comparison of the two numeric models for one sample of the heat exchanger showed the significant difference between the numeric temperatures which comes to 40 – 42%. It means the necessary for using the two–variables model because of the considerable influence on building of the velocity field.

The comparison of the decisions of the two heat exchanger samples which were modeled correspondingly on the two–variables model with the geometry of the two semi–channels showed some advantage of the first sample, which comes to 10% because of the smaller convective resistance of this sample. However for the whole volume of the heat exchanger the second sample will be more preferable because of the bigger heat transfer surface.

The values of the heat flows were chosen for the comparison of the experimental and numeric results because these values are the process characteristics. Both the experimental and numeric heat flows were calculated from the energy saving equation:

$$Q_i = m \cdot c_{Pi} \cdot \Delta T_i, \qquad (4)$$

here ΔT_i, Q_i, m_i, and C_{Pi} are the temperature difference, the heat flow, the mass flow and the

specific heat capacity of each heat carriers correspondingly.

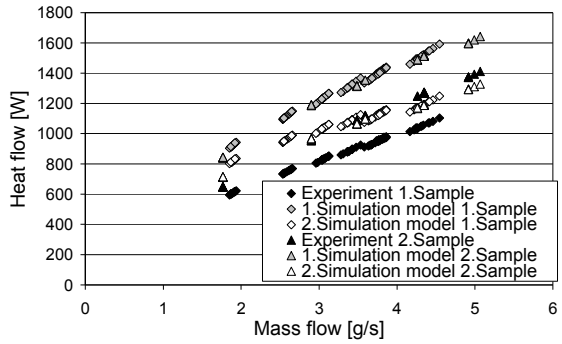

Figure 5. Experimental and numeric heat flow for the first heat carrier

The diagrams in Fig. 5 show the comparison between the experimental and numeric heat flux for the both samples of the first heat carrier.

Although the experimental heat flows of the both heat carriers are almost equal (the small difference about 3–5% between the values can be disregarded), the comparison between the numeric heat flows of the two mediums shows a significant difference which reaches about 20% for the one-variable simulation model.

It was suggested, that the reason for this big difference between experimental and calculated results of the heat exchanger outlet temperatures was connected with the irregular distributions of the temperatures and velocities. So, to study this problem, the two-dimensional model was solved.

The second model described above was changed for the investigation of the interior hydraulic and thermal fields for the both inlet cross–sections with the "direct opened" channels and with the "slotted" channels into a 2D-task. This numeric task was solved for 2 samples of the researched heat exchangers and for 2 other samples with channel widths 25% smaller than for the measured samples. Because of the difference of the inlet cross sectional geometry of the heat exchanger the numeric task is calculated for 2 geometries, each of which gives 2 independent solutions: the hydrodynamic and the thermal one. Figures 6 and 7 show the hydrodynamic and thermal fields of the primary (hot) heat carrier for the geometry of the first sample with the inlet values:

$$v_{in} = 3{,}7 \text{ m/s} \qquad T_{in} = 872 \text{ K}$$

The comparison of the numeric results for both the velocity and temperature fields shows a big difference between the hydraulic and thermal outlet values for the cross section of the "slotted" channels. The velocity and temperature distributions have a strongly expressed inhomogeneous character for the outlet cross section of the "slotted" channels and the expected homogeneous character for the outlet cross section of the "direct opened" channels. These Figures show a big hydraulic and thermal stress of the "slotted" channels for the middle cross section and for the outlet border.

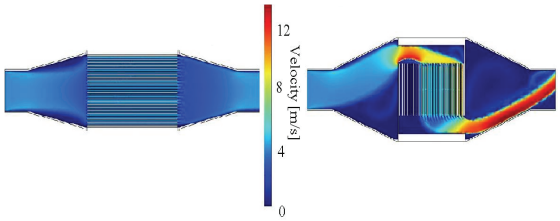

Figure 6. Velocity field in the direction of the „direct" channels (on the left) and in the direction of the „slotted" channels (on the right)

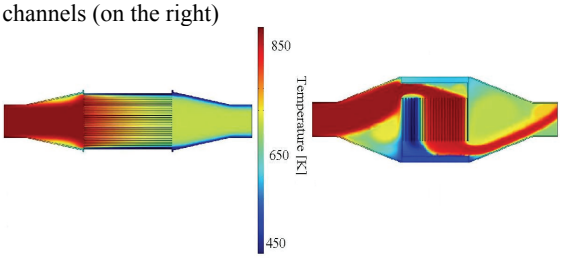

Figure 7. Temperature field in the direction of the „direct" channels (on the left) and in the direction of the „slotted" channels (on the right)

The analysis of the velocity and temperature fields in the "direct opened" channels for the two measured samples and for the two "virtual" samples with the channel's size 25% smaller (samples 1.1 and 2.1) than the real samples showed an increasing velocity and a decreasing temperature. The relative change was constant for both cases. The relative dimensionless difference between the numeric values was used for the comparison of the above presented results in the form of the equations (5):

$$\Delta_v = \frac{(v_{chan} - v_{in})_1 - (v_{chan} - v_{in})_2}{(v_{chan} - v_{in})_1};$$

$$\Delta_T = \frac{(T_{out} - T_{in})_1 - (T_{out} - T_{in})_2}{(T_{out} - T_{in})_1}, \qquad (5)$$

Here the indices *chan.*; *in* and *out* are corresponding to the values in the channel and on the inlet and outlet boundaries.

The data in the Table 3 shows the numeric results for the "direct opened" channels. The decreasing of the channel width gives an increasing velocity and a decrease of the outlet temperature. The comparison of these results is shown in the Table 4.

	Size of the channel [m]	Inside velocity [m/s]	Outlet temper. [K]
Sample 1.	2 / 0,8	4,52	645
Sample 1.1	1,5 / 0,8	4,81	597
Sample 2.	2,17 / 0,58	4,15	719
Sample 2.1	1,6 / 0,58	4,4	660

Table 3: Data for the "direct opened" channels

	Difference between the velocity [-]	Difference between the temperature [-]
Sample 1.- Sample 2.	0,45	0,33
Sample 1.- Sample 1.1.	0,26	0,18
Sample 2.- Sample 2.1.	0,36	0,28
Sample 1.1.- Sample 2.1.	0,37	0,23

Table 4: Dimensionless differences of the various geometries

The difference of the absolute values both the velocity and the temperature are shown above. The comparison of these data yields the largest difference between the data for the first and second samples, because both were changed: channel width and wall thickness. For the second sample the changing of the channel width gives the difference on the 10% bigger as for the first sample because of the higher sensitivity to structural changes. The difference between the data with the bigger value of the wall thickness is smallest.

4. Conclusions

The numeric results of the two-variables model correspond to the experimental results for both heat carriers better than the results of the one-variable model.

The divergence between the experimental and numeric values is bigger for the second heat carrier. This can be explained by the lower correspondence between the experimental and numeric inlet velocity values.

The experimental and numeric results show a significant advantage of sample 2 because of the finer structure. Although the advantage of sample 2 achieves 18% for the experimental results this value doesn't exceed 10% for the numeric results. This deviation indirectly confirms the influence of the inhomogeneous distribution of the velocity and temperature fields which could not be taken into account in the modeling with the 3D-geometry.

The numeric results of the 2D-model confirm the inhomogeneous distributions of both the hydraulic and the thermal characteristics of the "slotted" channels. The extreme inhomogeneity particularly in the inlet and outlet areas of the "slotted" channels brings a decrease of the active heat transfer surface.

The described numeric modeling can be used for further structure optimization similar heat exchangers.

Nomenclature:

u	Velocity
r	Variable value of the channel radius
R	Channel radius
x, y	Coordinate
m	Mass flow
D	Sample's diameter
c	Specific heat capacity
ε	Porosity
k	Heat transfer coefficient

Indices:

0	Inlet value
P	By the constant pressure
max	Maximal value
i	Number of the hear carriers

References:

[1] Th. Fend, W. Völker, R. Miebach, O. Smirnova, D. Gonsior, D. Schöllgen, P. Rietbrock: Experimental investigation of compact silicon carbide heat exchangers for high temperature, International Journal of heat and mass transfer 54 (2011), 4175 - 4181

[2] "Heat Transfer Module (User's Guide)", "Building and solving a Conduction and Convection Model," Heat Exchanger model for the COMSOL 3.4, p.78 – 85, 2006

[3] "Heat Exchanger Design Handbook" Vol.3 "Thermal and hydraulic design of heat exchangers" Paragraph 3.7.7, Hemisphering Publishing Corporation, 1983

[4] M. Khalil Bassiouny, Holger Martin: "Temperaturverteilung in parallelgeschalteten Kanälen von Platenwärmeaustauschern", Chem.–Ing.–Tech.57 (1985) Nr.4, S. 330-332

[5] LU Fang, LUO Young-Hao and YANG Shi-ming: „Analytical and experimental investigation of flow distribution in manifolds for heat exchangers", Journal of hydrodynamics 2008, 20(2): 179 – 185

[6] V. Ponyavin, Y.Chen, J.Cutts, M. Wilson, A.E. Hechanova: "Calculation of fluid flow distribution inside a compact ceramic high temperature heat exchanger and chemical decomposer", Journal of Fluids Engineering, June 2008, Vol.130/ 061104/1 – 8

[7] Zhen Hua Jin, Gi Tae Park, Yong Hun Lee, SoonHo Choi, HanShik Chung, HyoMin Jeong: „Design and Performance of pressure drop and flow distribution to the channel in plate heat exchanger", Eng. Opt., 2008 – International Conference on Engineering Optimization, Rio de Janeiro, Brazil, 01-05 June 2008